Available online at www.sciencedirect.com
ScienceDirect
Journal of the European Ceramic Society 27 (2007) 131–141
www.elsevier.com/locate/jeurceramsoc

Effect of porosity of cordierite preforms on microstructure and mechanical strength of co-continuous ceramic composites

Matteo Pavese [a,*], Massimiliano Valle [b], Claudio Badini [a]

[a] *Politecnico di Torino, corso Duca degli Abruzzi 24, 10129 Torino, Italy*
[b] *Petroceramics Srl, c/o PIONT, via Pasibio 3/5, 24044 Dalmine (Bg), Italy*

Received 20 November 2005; received in revised form 27 April 2006; accepted 6 May 2006
Available online 27 June 2006

Abstract

With the aim of reducing the overall cost of the process, co-continuous metal–ceramic composites were obtained by reactive metal penetration, starting from very low cost cordierite preforms. It was investigated how the preform porosity influences both the residual porosity left in the composites after infiltration and the mechanical properties. It was demonstrated that, despite a significant fraction of the initial porosity remains in the final composite, by a suitable choice of the preform composition and preparation method the mechanical properties are not much inferior than in the case of composites obtained from the much more expensive silica glass.

Keywords: Al_2O_3; Porosity; Mechanical properties; Co-continuous composites; Cordierite

1. Introduction

Co-continuous metal–ceramic composites consist of two interpenetrating continuous networks, one of a metallic alloy (generally an aluminium alloy) and one of a ceramic phase (generally alumina). They can be obtained by several techniques, one of the most interesting is reactive metal penetration (RMP), a particular type of reactive infiltration. It was firstly developed at Columbus University (Ohio, USA)[1–4]; afterwards, similar investigations were carried out in the USA,[5–17] Europe[18–26] and Asia.[27–32]

Composites obtained by RMP (also called C4, acronym for Co-Continuous Ceramic Composites) present an unusual set of properties, since the preparation method provides near net-shape components (the dimensional changes occurring during the reactive infiltration of preforms are very small, less than 1%) that may have a very high ceramic content (up to 80–85% in volume). These composites possess a continuous network of a metal alloy that provides good thermal and electrical conductivity, and of ceramic, that gives high stiffness, high hot strength and wear resistance.[2]

Reactive metal penetration is based on a displacement reaction between liquid aluminium and an oxide precursor; the latter must be able to undergo a reaction similar to the following one, concerning silica:

$$4Al + 3SiO_2 \rightarrow 3Si + 2Al_2O_3 \quad (1)$$

The silicon formed in the reaction dissolves in the aluminium melt, so that an Al–Si alloy is formed.

The main requirements in the choice of the precursor are:

- the reaction must be thermodynamically favoured;
- the precursor must not melt or change its geometrical shape at the reaction temperature (which is usually quite high, up to 1200 °C);
- the reaction should be fast enough to be economically interesting;
- the following equation must be satisfied:

$$\left(\frac{M}{dn_0}\right)_{\text{product}} \leq \left(\frac{M}{dn_0}\right)_{\text{preform}} \quad (2)$$

where M is the molecular weight, n_0 the number of oxygen atoms in the compound and d is the density. The meaning of this relationship is not immediately evident, however this relationship is fulfilled when the process involves a decrease of the volume of

* Corresponding author. Tel.: +39 011 564 4708; fax: +39 011 564 4699.
E-mail address: matteo.pavese@polito.it (M. Pavese).

0955-2219/$ – see front matter © 2006 Elsevier Ltd. All rights reserved.
doi:10.1016/j.jeurceramsoc.2006.05.080

the ceramic. For instance in the case of silica infiltration, reaction (1), keeping in mind that silica density is around 2.2 g/cm^3 and alumina density is around 4 g/cm^3, it is possible to write these correspondences:

$$1\,\mathrm{cm^3\,SiO_2} \rightarrow\ 2.2\,\mathrm{g\,SiO_2} \rightarrow\ 36.7\,\mathrm{mmol\,SiO_2} \rightarrow\ 24.5\,\mathrm{mmol\,Al_2O_3} \rightarrow\ 2.49\,\mathrm{g\,Al_2O_3} \rightarrow\ 0.62\,\mathrm{cm^3\,Al_2O_3} \quad (3)$$

The volume reduction happens at a microscopic level, so that no macroscopic dimensional changes occur in the preform. Simply, the voids created by the transformation of SiO_2 into Al_2O_3 are filled with liquid aluminium. In this way the liquid metal can always have access to fresh precursor, and the reaction can proceed through the whole preform body.

The value of $\frac{M}{dn_0}$ for alumina is rather low, so that almost any oxide can be infiltrated by aluminium.[18]

By using different materials, different composite compositions results; as seen in Eq. (4), for instance, if cordierite is used as a precursor, some spinel ($MgAl_2O_4$) forms in addition to alumina:

$$20Al + 3Mg_2Al_4Si_5O_{18} \rightarrow\ 6MgAl_2O_4 + 10Al_2O_3 + 15Si \quad (4)$$

Moreover, depending on the composition and density of the preform, different ceramic content are obtained in the final composite, as shown in Table 1.

The potential of reactive metal penetration in industry has not been completely investigated yet. Widespread applications for the processing of wear-resistant components are foreseeable, provided that a good compromise between cost and properties is achieved.

Until now the most important precursor used in C4 manufacturing has been pure silica glass,[2–4,18–31] which is a relatively expensive starting material (the commercial price of silica glass is of several tens of euros per kilogram); however, it was already shown[7,12,14,15,33,34] that mullite, cordierite or other silicates can be used as precursors for the preparation of C4. It is also possible to insert a second phase into these preforms in order to tailor some features of the final product.[23]

Recently it was demonstrated[33] that a commercial product based on cordierite and mullite could be used as a preform for the preparation of composites with interesting properties. This preform has a much reduced price with respect to silica glass (1–2 €/kg) and so could be used to enhance the chances of an industrial development of C4. The mechanical properties of such composite were studied, and it was made evident that the porosity of the preform had a very strong effect on the properties of the produced composite. The relationship between the porosity of the preform and that of the composite, though, was not investigated, nor the mechanism by which the infiltration advances. Moreover, the starting materials contained both cordierite and mullite, so that any consideration about the mechanism was complicated by the composite structure of the preform itself.

This paper is aimed at preparing and characterising co-continuous ceramic/metal composites obtained from commercially pure cordierite preforms with variable porosity; two different production methods for these preforms were investigated, extrusion and pressing, both widely used in industrial routine, that provide low cost items (in both cases the commercial price is few euros per kilogram). The goal of the work was to assess the relationship between preform and composite porosity, to measure the mechanical behaviour of these composites, and to better investigate the mechanism of infiltration in the case of porous preforms.

2. Experimental procedure

The preforms used as precursors in this work were supplied by Petroceramics Srl (Milano, Italy), and consist of commercially pure cordierite ceramics, obtained by two methods. The first kind of preform is prepared by uniaxial pressing of atomised powders and subsequent sintering (referred to as "pressed cordierite"); the second type of preform is obtained by extrusion and sintering ("extruded cordierite").

These materials are industrially prepared starting from kaolin, talc, clay and alumina.

In the case of pressed cordierite, a suspension of fine powder is sprayed in a hot gas flux, in order to obtain hollow granules of roughly spherical shape with a diameter between 100 and 150 μm. These granules are then uniaxially pressed and sintered at 1290 °C. Three samples have been investigated (P1–P3), which have been pressed at different pressures (20, 12 and 8 MPa) and differs essentially for their porosity content and pore distribution.

In the case of extruded cordierite preforms, the production process consists in the preparation of a slurry of fine powders of the precursors of cordierite, followed by extrusion and sintering at 1340 °C. Different porosity is obtained by varying the slurry composition, in particular by the addiction of sawdust. A sample (E1) has been obtained without sawdust, while other ones (E2, E3) have been realised from a slurry containing an increasing amount of such component; the wood, as the binder, burns away during the heat treatment.

Table 1
Theoretical characteristics of C4 obtained from different ceramic preforms

Preform	Formula	Preform density (g/cm^3)	Theoretical C4 composition			Theoretical C4 density (g/cm^3)
			Al_2O_3 (%)	$MgAl_2O_4$ (%)	Al (%)	
Silica	SiO_2	2.2	62.2	–	37.8	3.48
Mullite	$Al_6Si_2O_{13}$	3.2	84.0	–	16.0	3.75
Cordierite	$Mg_2Al_4Si_5O_{18}$	2.6	38.2	35.2	26.6	3.49

Some comparison were made with materials studied in previous works, in particular with composites obtained from the already mentioned commercial cordierite-mullite perform,[33,35] from sintered cordierite glass,[33–35] and from silica glass.[2,23,32] In these works it was demonstrated that it is not essential to use silica glass, the most expensive preform, in order to realise C4 composites with interesting mechanical properties. In particular it was proved the possibility of using cordierite, even if the infiltration mechanism was probably slightly different than in the case of silica. Moreover, commercial preforms were used revealing the possibility of employing very cheap materials to prepare C4 composites. The study of the effect of the porosity of the preform on the properties of composites was however necessary since cheap commercial preforms tend to be very porous.

To obtain C4 composites the preform (a whatever preform among those mentioned above) was inserted in a molten aluminium bath (99.9% pure, from Aldrich), kept at the temperature of 1200 °C, for a time ranging from 20 min to 4 h, then the bath was cooled up to 850 °C and the composites were extracted and cooled in calm air. The infiltration procedure carried out is reported with more detail in a previous work.[23] The bath temperature was chosen in order to achieve the best infiltration rate and a regular composite microstructure: a lower infiltration temperature slows down the reaction,[35] while a too high temperature can bring to a more inhomogeneous structure.[27]

The precursors were analysed with Differential Thermal Analysis (Perkin-Elmer DTA 7) in order to establish their melting point.

Both precursors and composites microstructures were investigated by using several techniques. The composition was assessed by X-ray diffraction (Philips PW3040, equipped with a monochromator, Cu Kα radiation) and EDS measurements (Oxford 7353). Density and porosity measurements were also carried out (electronic balance equipped for density measurement with displacement method, picnometry, Carlo Erba PO2000 Mercury Intrusion Porosimeter with macropores unit).

Three types of porosity were measured: bulk density and apparent density by hydrostatic methods[36] on parallelepipedal samples, and powder density by water picnometry[37] on crushed powder. Bulk density is the weight for unit volume of a solid material, so that it keeps into account the contribution of all pores, both open and closed; apparent density is the ratio between the mass of the dry specimen and its apparent volume, so that only the closed pores are considered; powder density represent the theoretical density of the solid material, since it is hypotesised that after crushing no closed porosity is retained in the powder.

From apparent density and bulk density it is possible to derive the closed and open pore fraction, following the equations:

$$p_{\text{open}} = 1 - \frac{d_{\text{bulk}}}{d_{\text{app}}}, \qquad p_{\text{tot}} = 1 - \frac{d_{\text{bulk}}}{d_{\text{theor}}},$$
$$p_{\text{clos}} = p_{\text{tot}} - p_{\text{open}} \tag{5}$$

where p_{open}, p_{clos}, p_{tot} are respectively the open, closed and total porosity, and d_{bulk}, d_{app}, d_{theor} are respectively the bulk, apparent and theoretical densities. For our calculations powder and theoretical density were considered equal.

Morphology was also investigated by optical and SEM microscopy (respectively Reichert Young MF3 and LEO 1450 VP). The composite mechanical properties were investigated in terms of elastic modulus and flexural strength. Young modulus was measured (GrindoSonic MK5 instrument) exploiting a method based on the analysis of the transient natural vibration following an impulse excitation. Flexural strength by three-points bending tests (Sintech 10D equipment, stroke control with crosshead speed of 0.1 mm/min; the sample size was 50 mm × 10 mm × 3 mm, the distance between the supports 40 mm); a mean of a minimum of four values was used in each case. Co-continuity of the composites was verified both by microscopy observation and by leaching the metallic phase by means of concentrated hydrochloric acid and verifying the mechanical cohesion of the remaining ceramic network.

3. Results and discussion

3.1. Cordierite preforms characterisation

The cordierite preforms were initially characterised in order to asses their composition and structure. Their composition is reported in Table 2.

Each family of samples (P1–P3 and E1–E3) gives substantially the same results, both relatively to phases present and EDS elemental analysis. Moreover, the XRD analysis confirms the composition data; in E1–E3, where some cristobalite (SiO_2) is present, there is a higher content of silicon, in P1–P3, where mullite is the secondary phase instead of spinel, less magnesium is observed. It must be noted that pressed cordierites present a higher impurity content than extruded ones.

The porosity of these preforms has been calculated from density; by measuring geometrical, apparent and true density, total, open and closed porosity have been evaluated. These data are collected in Table 3.

It is evident that pressed cordierites provide a lower porosity, while very high values of porosity arise from the extrusion

Table 2
Elemental and phase composition of pressed and extruded cordierite preforms

Preforms	Phases present (in brackets minority phases)	Composition (wt.%)				
		Si	Al	Mg	K	Na
P1–P3	Cordierite, mullite (alumina, spinel)	40.5	40.9	15.3	0.8	2.5
E1–E3	Cordierite, spinel (cristobalite)	43.8	34.3	21.0	0.1	0.8

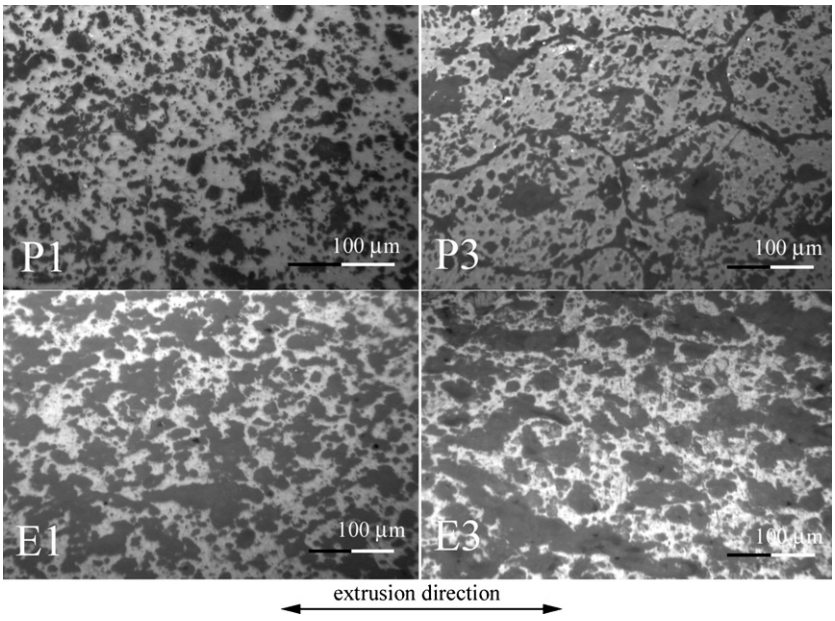

Fig. 1. Porosity of cordierite preforms P1, P3, E1 and E3.

method, when sawdust is inserted in the slurry. In each method, the less porous samples present a higher degree of closed porosity, while the more porous ones have almost only open porosity. The picnometry density of all samples is similar, save for E1. A possible explanation of this phenomenon will be given in the following.

In Fig. 1 some micrographs of the samples P1, P3, E1 and E3 are reported. From a microstructural analysis of the preforms two particular pieces of information are taken. A comparison between samples P1 (Fig. 1a) and P3 (Fig. 1b) shows that the latter underwent a very poor sintering, due to the low applied load in the pressing stage. Long pores between the granules are yet present, and the central void is also retained after sintering. Samples P1 and P2 does not present these defects (Fig. 2).

Samples E1 (Fig. 1c) and E2/E3 (Fig. 1d) also present a different structure: in all extruded cordierites the porosity is partially aligned along the extrusion direction; this phenomenon however is particularly evident in the samples that contain some sawdust: during the extrusion the wood fragments (that have a high shape factor) partially orientate along the extrusion direction, leaving, after heat treatment, large and elongated pores.

The pores distributions are presented for the samples obtained by extrusion; in this case the presence of the pores derived from sawdust is particularly evident: in the sample E1, prepared

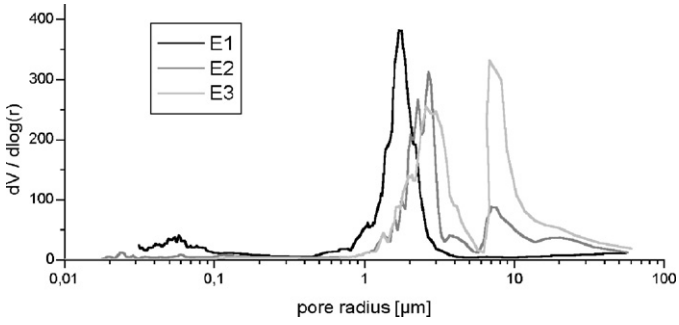

Fig. 2. Pore distribution of extruded cordierite preforms.

without wood, a single peak is observed at a couple of micrometers, while in samples E2 and E3, where wood was present, is observed the appearance of a second peak, more intense for the more porous sample, at higher pore size (7–10 μm); it is thought that these pores were left during the burning out of the wood. It must not be forgotten that the porosimetry measurements on oriented pores show the smaller pore dimension, so that very long pores with small cross-section are seen at the pore size of the section.

Before carrying out the infiltration procedure, the behaviour of the preforms at the infiltration temperature was investigated.

Table 3
Density and porosity of the different cordierite preforms

Precursors	Geometric density (g/cm^3)	Apparent density (%)	Picnometry density (%)	Total porosity (%)	Open porosity (%)	Closed porosity (%)
P1	2.27	2.29	2.54	12.7	1.0	11.7
P2	2.13	2.41	2.56	17.9	11.3	6.6
P3	2.07	2.50	2.56	20.4	17.0	3.4
E1	2.01	2.26	2.49	22.5	11.0	11.5
E2	1.70	2.36	2.57	34.4	27.8	6.6
E3	1.46	2.53	2.58	43.9	42.3	1.7

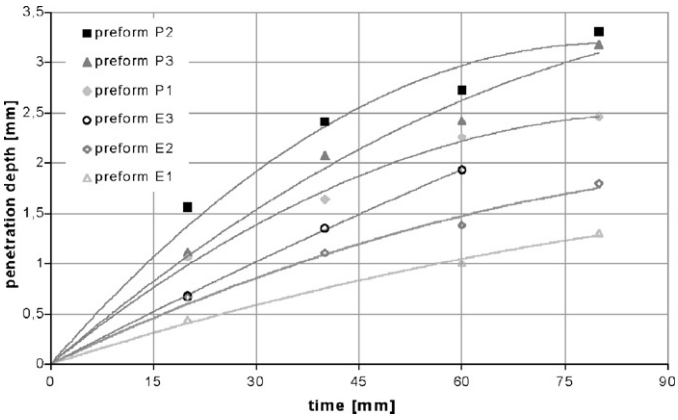

Fig. 3. Infiltration kinetics for the different cordierite preforms.

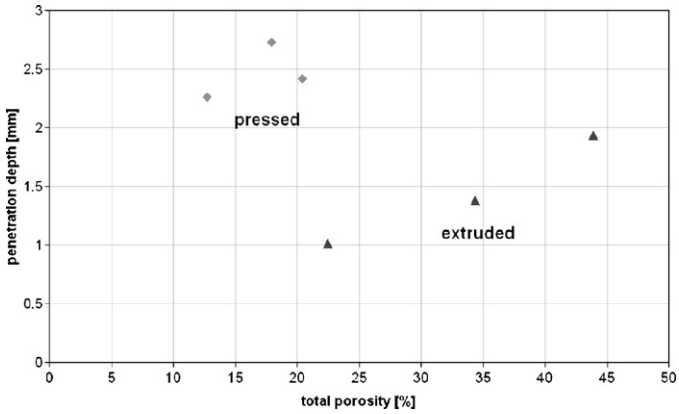

Fig. 4. Penetration depth as a function of porosity after 60 min of infiltration for the different cordierite preforms.

DTA measurements were carried out and the melting point of all the cordierite preforms was found to be higher than 1330 °C. Finally, a prolonged heat treatment (8 h) at 1200 °C was performed and neither change in size nor deformation were observed in any of the cordierite preforms.

3.2. Composite processing and characterisation

Infiltration rate measurements were carried out by checking infiltration depth after reaction times between 20 and 80 min, in order to evidence the effect of porosity on the infiltration rate. The results are plotted in Fig. 3.

The results are not consistent with data on silica-derived C4 composites,[23] where the porosity seemed to slow down the infiltration. Here, instead, it seems that the infiltration rate increases with total porosity, as shown in Fig. 4 for 60 min of infiltration. Excluding sample P3, whose structure is characterised by a low sintering, a rising trend is observed both for extruded and for pressed samples, even if it is clear that pressed cordierites are infiltrated much faster than the extruded ones. It is likely that the elongated shape of the pores in extruded cordierites may slow down the infiltration reaction with respect to pressed samples.

More easy is the interpretation of the structure and composition data of the composites obtained after infiltration. In a first step, XRD analyses were carried out. The main components in these composites were, as expected, an Al–Si metal alloy, alumina and $MgAl_2O_4$ spinel, constituting the ceramic phase.

As shown in Fig. 5, however, some other phases were found; in samples P1–P3 the main one was a sodium hexaaluminate ($NaAl_{11}O_{17}$), probably derived from the sodium present in the preform, whilst in samples E2 and E3 aluminium nitride was found in appreciable quantity. The presence of AlN was completely unexpected, since at a first glance there was no reason why a nitride could be formed during the reaction; however, it is possible that during the burning of the wood (used in the preform to increase the porosity) some oxynitride or nitride could be formed; on the other hand it was previously observed[23] that AlN can form from the reaction between silicon nitrides or oxynitrides and aluminium. This explanation could also give reason for the lower theoretical density of E1 preforms with respect to E2 and E3. Since silicon and aluminium nitrides have a density value around 3.3 g/cm^3, higher than cordierite, the presence of nitrides could raise the overall preform density.

The presence of AlN is potentially harmful for this kind of materials, since it is well known that it can react with humidity

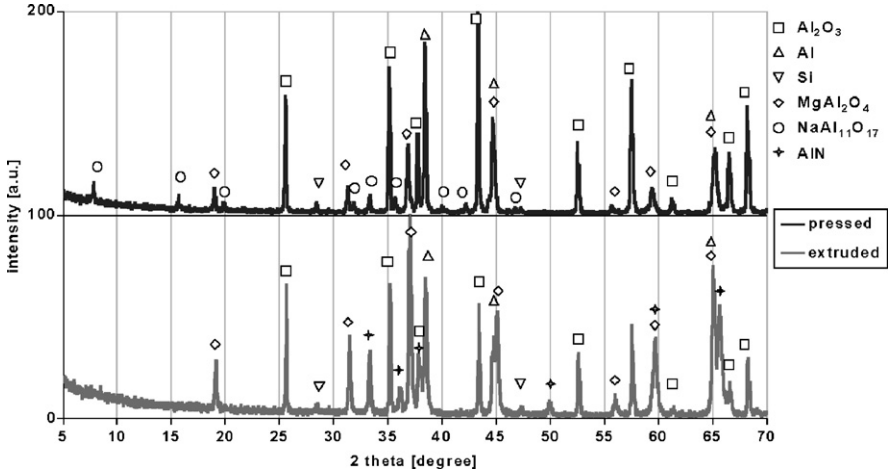

Fig. 5. X-ray diffraction spectra for composites obtained from pressed or extruded preforms.

according to the reaction:

$$2AlN + 3H_2O \rightarrow Al_2O_3 + 2NH_3 \quad (6)$$

The formation of ammonia was evident by the smell and it was also proved by immersing the samples E2 and E3 in water and measuring the pH; small bubbles immediately formed following immersion, and after 30 min the pH had exceeded 10, bearing out the formation of a basic compound.

Even if the samples come into contact with water during their preparation (cutting and polishing operations), the reaction (6) does not seem to influence in a significant way the mechanical properties of the composites; the strength data of E2 and E3 samples are consistent with other cordierite ones, where aluminium nitride is not present. It is likely that the reacting AlN is on the surface of the open pores, those exposed to humidity, so that the development of gases inside the material does not bring to mechanical decohesion of the sample.

By microscopic observations on the composites, three different zones, characterised by a different microstructure, were observed. Going from the external part (the first to be infiltrated) towards the core of the samples, it is possible to individuate a first zone characterised by roughly spherical grains of ceramic (lighter), surrounded by a metal network (darker), linked at their borders to form a co-continuous three-dimensional structure (Fig. 6a); this microstructure is similar to that observed in silica-derived C4 composites, even if in the silica case the three-dimensionality of the structure is more pronounced. In general, all preforms containing only Si, Al and O (silica, mullite, sillimanite, . . .) present, after infiltration, a microstructure of this type, where the metal alloy percentage is depending on the initial composition of the preform (as seen also in Table 1: the more Al in the preform, the less metal alloy in the final composites). When other elements (in the preform, as Mg in cordierite, or impurities, as Na, K or Ca in commercial materials) are present the microstructure of C4 composites is different.

In this case, where both Mg from cordierite and some impurities (mainly K and Na) are present, there is a change in the microstructure going toward the inner part of the samples. The structure shown in Fig. 6a slowly gives way to a different microstructure type, where it is intermingled with a zone of smaller grain size, which appear of uniform dark grey at SEM observation (Fig. 6b). This latter microstructure becomes more and more common going toward the centre of the sample (Fig. 6c). In addition, in the composites obtained from pressed preforms, probably due to the higher impurity content, also a needle-shaped structure was detected in the centre of the sample by using optical microscopy (Fig. 6d); in this case lighter phase is Al and darker one is $NaAl_{11}O_{17}$.

In the composites obtained from extruded preforms, this last kind of microstructure lacks, and only a structure similar to the one observed in Fig. 6b–c is present in the central part of the samples.

To investigate the chemical and phase composition of these different zones, EDS analyses were carried out. A compositional map of a zone similar to that in Fig. 6b and c is presented in Fig. 7. It is evident that the zones that appear dark in the SEM micrograph (characterised by the finer microstructure) are richer in magnesium (in the form of spinel), while the lighter ones are alumina grains. It is possible to see also some aluminium alloy zone intermingled with both alumina and spinel grains, where neither oxygen nor magnesium are present. This suggests that, at the end of the infiltration process, the magnesium react to form spinel and does not remain dissolved into the metal in a

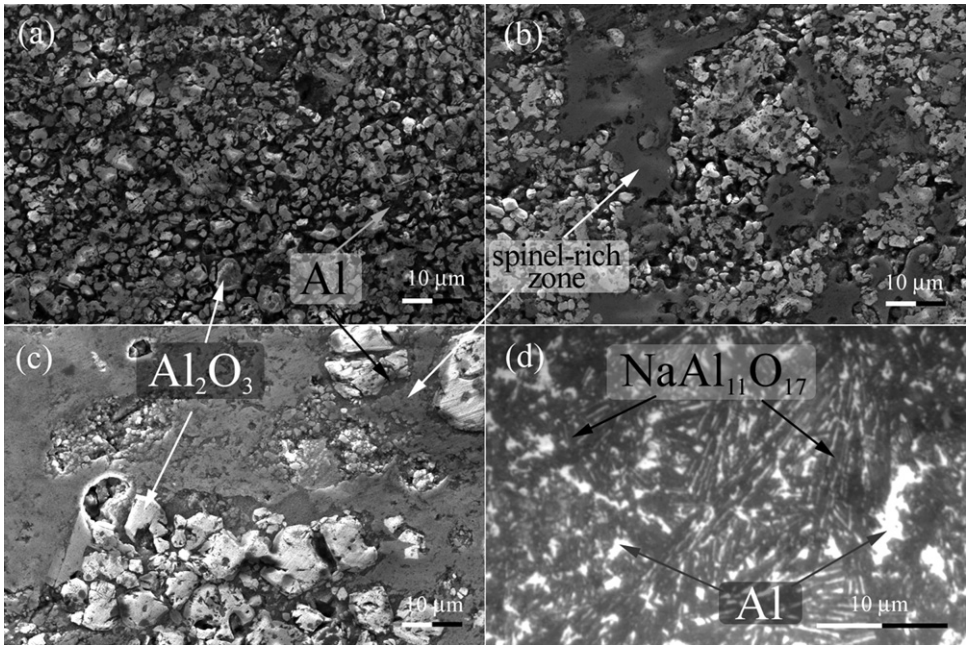

Fig. 6. Microstructure of composites obtained from cordierite preforms: external zone (a); intermediate zone (b); internal zone (c) (SEM micrograph: Al_2O_3 is lighter and Al alloy is darker; the larger dark zones are rich in $MgAl_2O_4$); central part of samples obtained from pressed preforms (d) (optical micrograph: here the ceramic phase is darker, and the metal alloy is lighter).

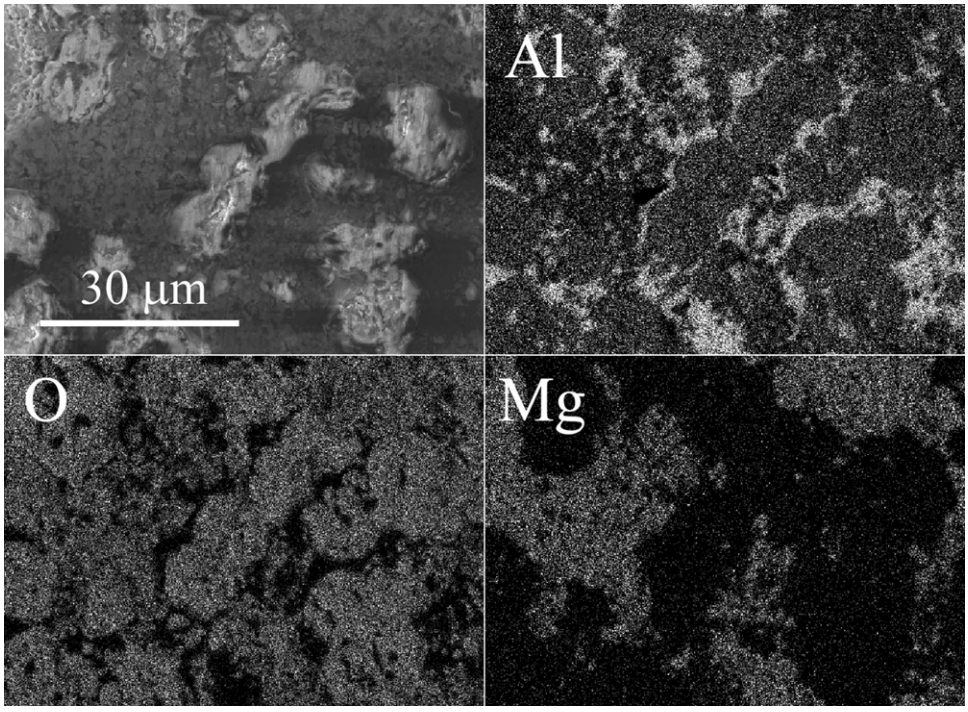

Fig. 7. Microstructure and compositional maps of Al, O, Mg in a zone comprising Al, Al_2O_3 and $MgAl_2O_4$ phases.

significant quantity. This is confirmed both from thermodynamical calculations[23] and from EDS measurements on the metal alloy in the composite, where no more than 1% magnesium in present.

In the central part of the pressed samples, the last to be infiltrated, some XRD analyses were performed, in order to determine the composition of the needle-shaped zones. Hexaaluminate peaks in the centre of the composite are much higher than in outer parts, suggesting that Na (and K) impurities accumulate in the last infiltrated zone. EDS measurements performed on wholly and partially infiltrated samples confirm these hypotheses, showing an accumulation of both sodium and potassium on the infiltration front.

It must be noted that in composites obtained from extruded cordierites, where the impurity content is much lower, the hexaaluminate phase is not present, and no needle-shaped structure is observed at the microscope, giving an additional confirmation that its presence is essentially linked to the alkaline elements.

Also magnesium is partially drawn away from the surface of the sample during infiltration, since in the external layer (Fig. 6a) only alumina and aluminium are present, while magnesium is present as spinel only in the dark zones shown in Fig. 6b and c that are absent on the surface. An explanation for this phenomenon is the following: when cordierite reacts with aluminium, there is an local enrichment of magnesium on the reaction front. When the concentration of magnesium increases over a certain limit, spinel is formed. At the beginning of the infiltration, since no magnesium is present in the infiltrating alloy, no spinel precipitation is detected. After a significant quantity of cordierite has reacted, however, i.e. in the inner part of the sample, the concentration of magnesium is sufficient and spinel is observed.

The observation of the partially infiltrated samples leads also to some considerations about the infiltration mechanism that will be further strengthened by the porosimetric analyses. As shown in Fig. 8, the reacted zone (on the left in the images) clearly presents less pores than the preform; thus it seems that during the infiltration a significant fraction of the porosity is filled.

This reduction of the porosity during the infiltration is confirmed by comparing density of preforms and composites (Table 4).

In all cases the porosity diminishes, in a more evident way in the samples with higher preform porosity. On the contrary the quantity of closed porosity generally increases, as already observed in a previous work.[33] The effect of infiltration thus seems to be the reduction of the total porosity and the increase of the closed porosity fraction, which means that molten aluminium

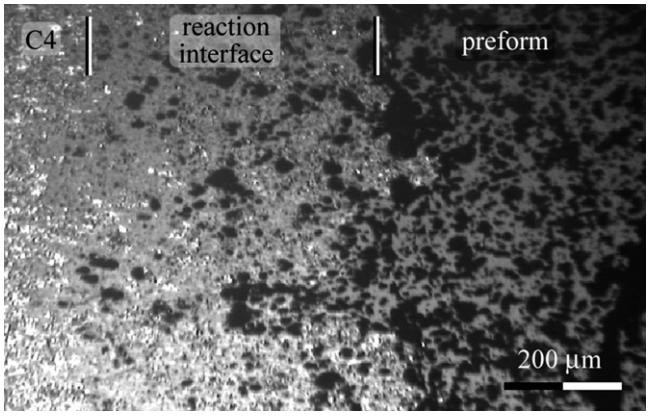

Fig. 8. Porosity of partially reacted samples, showing the reaction interface and the different porosity content of preform (right) and composite (left).

Table 4
Comparison between the porosity of cordierite preforms and of the composites obtained from their infiltration

Precursors	Preform			Composite			Total porosity reduction (%)
	Total porosity (%)	Open porosity (%)	Closed porosity (%)	Total porosity (%)	Open porosity (%)	Closed porosity (%)	
P1	12.7	1.0	11.7	9.3	1.2	8.1	26.8
P2	17.9	11.3	6.6	13.0	2.4	10.6	27.4
P3	20.4	17.0	3.4	12.2	8.5	3.7	40.2
E1	22.5	11.0	11.5	15.4	2.9	12.5	31.6
E2	34.4	27.8	6.6	19.0	10.2	8.8	44.8
E3	43.9	42.3	1.7	27.7	22.9	4.8	36.9

infiltrates open pores and, at last partially, closed pores as well; however, owing to the volume reduction of ceramic part of the sample occurring during the process, a residual closed porosity can not be avoided.

As shown by porosimetry, the mean pore dimension is also reduced. In Fig. 9 are presented the case of sample P2 and P3. The first represents the samples P1, P2, and E1, where a strong reduction of pore size is observed. The second represents the case of samples P3, E2, and E3, where bigger pores were present in the preform, and where the size reduction is less evident. This difference, together with the fact that the porosity reduction in samples P3, E2 and E3 is higher than in the other ones, is likely to be due to the presence, in these preforms, of pores with high shape factor. As a consequence of the different behaviour of P2 and P3 samples, also the P1–P2–P3 relative porosity trend for composites results different from that of the preforms shown in Table 2.

From all these data some general considerations about the reactive penetration process can be drawn, even if a deeper study of the reaction front would be needed in order to determine the microscopic phenomena that control the reaction between aluminium and cordierite. Some pieces of evidence however can be recorded:

- the infiltration rate mainly depends on the method of production of preforms, and to a lesser degree from the amount, size and shape of pores, whose presence seems to slightly speed up the reaction;
- the infiltration reduces the total porosity;
- the closed porosity increases;
- pores are reduced in size during the infiltration;
- there is a reaction zone where, as evidenced by XRD analysis on partially reacted samples, both products and reactants are present;
- sodium and potassium impurities are drawn toward the centre of the sample;
- the reaction zone enriches in sodium and potassium during the proceeding of the reaction, so that the microstructure is modified in the middle part of the sample if a sufficient impurity degree is present.

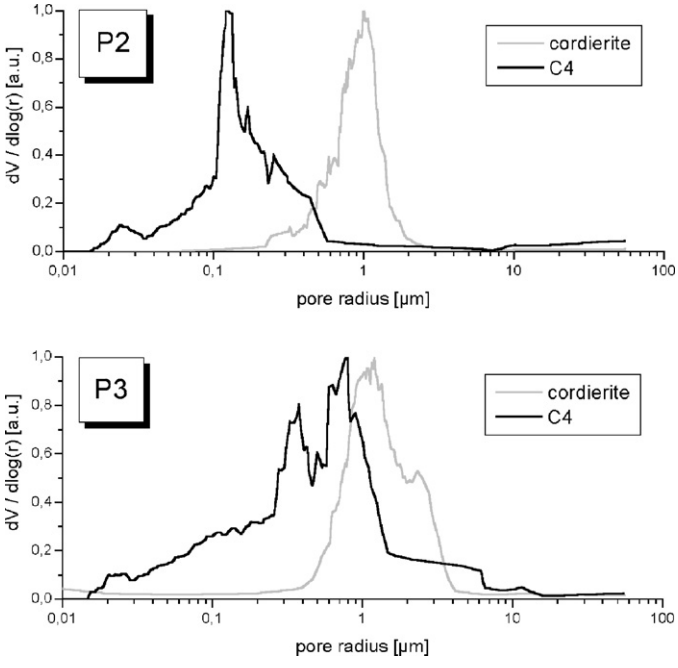

Fig. 9. Pore distribution of composites obtained from preforms P2 and P3.

Finally the obtained composites were characterised from a mechanical point of view. Young's modulus and three point bending tests were performed; the results are shown in Table 5 and, plotted against porosity, in Fig. 10.

From this figure it is immediately evident that, with the exception of sample P3, both Young's modulus and flexural strength increase with decreasing porosity. The best results are obtained with sample P1, that present a Young's modulus of 157.6 MPa and a flexural strength of 244 MPa, better values than those obtained in previous works on composites from cordierite performs,[33–35] and not so far from the values for silica-derived cordierites.

Table 5
Mechanical properties of composites obtained from the different cordierite preforms

Preform	Total porosity (%)	Young's modulus (GPa)	Flexural strength (MPa)
P1	9.3	157.6	244
P2	13.0	148.5	234
P3	12.2	127.5	172
E1	15.4	133.0	210
E2	19.0	124.7	176
E3	27.7	95.1	111

Table 6
Comparison between mechanical properties of composites obtained from different types of preforms

Preform	Composite total porosity (%)	Young's modulus (GPa)	Flexural strength (MPa)
Silica[2,23,32]	<1	200–210	260–470
Dense cordierite[33–35]	11.5	157	186
ICRAConcept C2 cordierite[33,35]	17.5	116	140
P1, this work	9.3	157.6	244
E1, this work	15.4	133.0	210
E2, this work	19.0	124.7	176

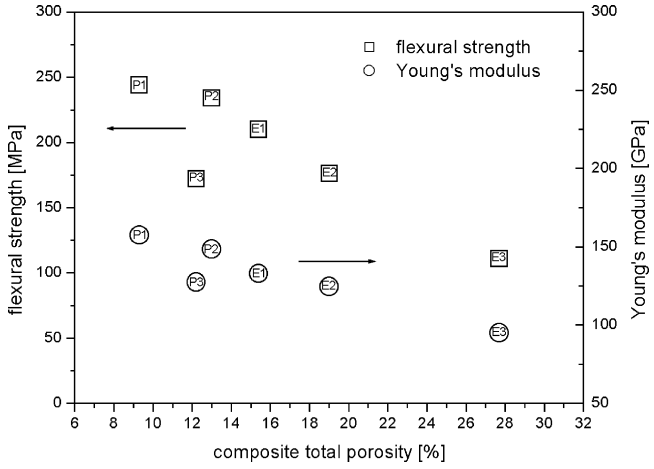

Fig. 10. Flexural strength and Young's modulus for the composites obtained from the different cordierite preforms.

The trend of Young's modulus and flexural strength is close to the linearity with respect to porosity, as predicted by the literature models[38]; also in the case of samples E, derived from cordierites obtained by extrusion, the shape factor of the pores after infiltration is rather close to unity, so that no significant pore shape effect is observed on Young's modulus and strength.

The case of sample P3 is different from the others, since the cordierite P3 is not wholly sintered, and large pore occurs, whose size is not substantially reduced after infiltration, as shown in Fig. 9. At the end of the infiltration the P3 sample result with a slightly lower porosity than sample P2, but larger elongates pores are present, similar to those observed in the cordierite (Fig. 1). The presence of pores with high shape factor has a marked effect on the mechanical properties,[38] a negative one if they are misaligned with respect to the applied stress. It is probable that the marked decrease in mechanical properties observed for composites P3 is to ascribe to the presence of this kind of pores.

A comparison with C4 composites obtained from different preforms is presented in Table 6. From the materials prepared in this work P1 sample has been chosen since it presents the best mechanical properties, E1 and E2 since their porosity is comparable with that of ICRAConcept C2.[33]

It is evident that the best performance is given by the composite obtained from silica glass, the difference being particularly evident for the Young's modulus. This is easily explained by the fact that in composites obtained from silica glass the ceramic

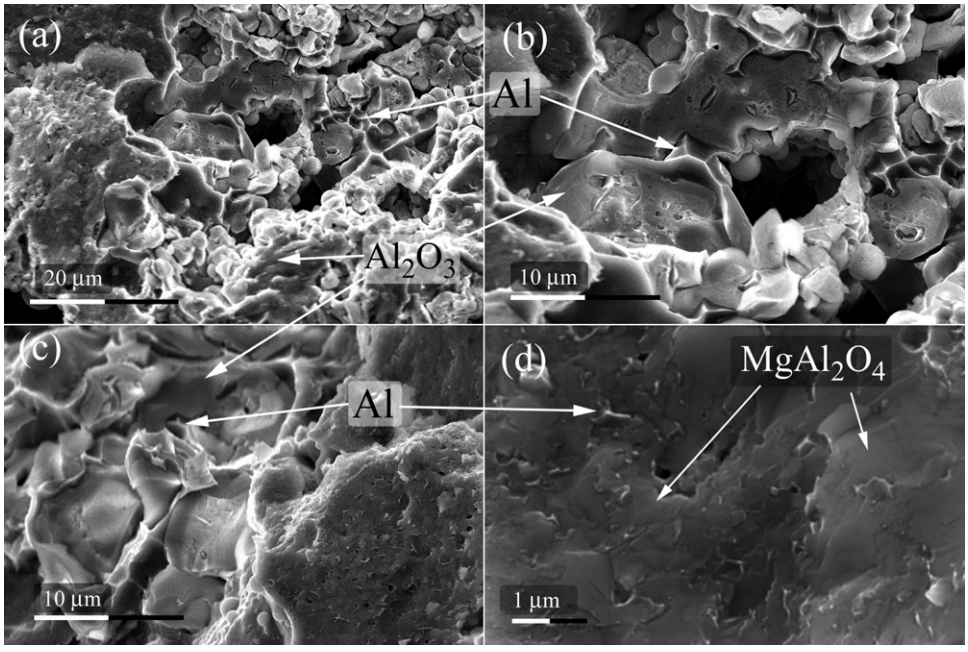

Fig. 11. Fracture surfaces of the external (a, b) and internal (c, d) zones in the composite obtained from pressed cordierite P1; the magnifications show the ductile behaviour of the metal network.

phase is made only by alumina, while in the composites obtained from cordierite also spinel is present, which shows a Young's modulus lower than alumina. The bending strength of the P1 sample instead is close to the inferior limit for silica-derived C4.

It is interesting to note that samples E1 and E2, although similar in porosity to the composite obtained from ICRAConcept C2,[33] present higher mechanical strength. Since ICRAConcept C2 is made from mullite grains inserted in a cordierite matrix, and is known that mullite-derived C4 have high modulus and strength,[35] the opposite could be expected. However, as it was observed with sample P3, the porosity shape plays an important role in determining the mechanical properties, and the low modulus and strength of composites obtained from ICRAConcept C2 can be ascribed to the presence of big elongated pores.

C4 composites obtained from P1 cordierite preforms has similar modulus than composites obtained from fully sintered cordierite glass powders, but the mechanical strength is much higher. It is likely that this is due to the high impurity content of sintered cordierite powders.[33,35] Since the preforms used in this work have an impurity content lower than those obtained from sintered cordierite glass, the mechanical strength of the composites is higher.

The different types of microstructures observed in C4 composites correspond to different features on the fracture surface. In Fig. 11, the fracture surface of both the external aluminium/alumina zone (Figs. 6a and 11a and b) and the "dark" zone (Figs. 6b and c and 11c and d, containing spinel) are presented. In the two cases both ductile (aluminium alloy) and brittle (alumina or spinel) zones are visible; where the standard co-continuous microstructure is observed, however, the scale of aluminium ligaments is bigger than in the zones containing spinel, suggesting that these last perform worse as far as the toughness is concerned, since is known in the literature[39] that a too small dimension of the metal ligaments bring to a lower toughening effect on the composite.

4. Conclusions

In this paper co-continuous ceramic composites were realised starting from commercial cordierite items, obtained by sintering pressed or extruded powders, by reaction metal penetration technique.

The preform preparation method greatly influences its characteristics, in terms of porosity and pores shape and dimension, and brings to different infiltration kinetics and to different properties of the final product. Due probably to the lack of elongated pores, the preforms obtained by pressing are infiltrated at a higher rate than those obtained by extrusion; in both cases, however, the pores quantity has a beneficial effect on the infiltration rate. The infiltration process always reduces both the porosity and the pore size, and yield a prevalent closed type porosity.

The best mechanical behaviour (stiffness and flexural strength) of the composites is obtained by infiltrating the preforms obtained by pressing, probably due to their lower residual porosity. The presence of impurities however seems to play an important role on the microstructural and mechanical characteristics of the C4. The impurities are repelled from the infiltration front and thus they concentrate in the heart of the composite, where they give rise to specific phases and microstructures.

The mechanical properties of the obtained composites are inferior to those of silica-derived C4, however, the difference is not extremely conspicuous, and since the cost of silica glass preforms is higher by an order of magnitude than that of cordierite preforms, it is thought that the use of such materials could lower in a very significant way the final cost of these composites.

References

1. Breslin, M. C., Process for preparing ceramic–metal composite bodies. U.S. Patent 5214011, 25 May 1993.
2. Breslin, M. C., Ringnalda, J., Xu, L., Fuller, M., Seeger, J., Daehn, G. S. *et al.*, Processing, microstructure, and properties of co-continuous alumina–aluminum composites. *Mater. Sci. Eng. A*, 1995, **195**, 113–119.
3. Xu, L., The deformation and fracture of co-continuous alumina–aluminum composites under monotonic and cyclic loading. PhD thesis, Ohio State University, Columbus, OH, 1994.
4. Daehn, G. S., Starck, B., Xu, L., Elfishawy, K. F., Ringnalda, J. and Fraser, H. L., Elastic and plastic behaviour of a co-continuous alumina/aluminium composite. *Acta Mater.*, 1996, **44**, 249–261.
5. Gao, Y., Jia, J., Loehman, R. E. and Ewsuk, K. G., Transmission electron microscopy study of Al/Al_2O_3 composites fabricated by reactive metal infiltration. *J. Mater. Res.*, 1995, **10**, 1216–1225.
6. Gao, Y., Jia, J., Loehman, R. E., Ewsuk, K. G. and Fahrenholtz, W. G., Microstructure and composition of Al–Al_2O_3 composites made by reactive metal penetration. *J. Mater. Sci.*, 1996, **31**, 4025–4032.
7. Ewsuk, K. G., Glass, S. J., Loehman, R. E., Tomsia, A. P. and Fahrenholtz, W. G., Microstructure and properties of Al_2O_3–Al(Si) and Al_2O_3–Al(Si)–Si composites formed by in situ reaction of Al with aluminosilicate ceramics. *Met. Mater. Trans. A*, 1996, **27**, 2122–2129.
8. Fahrenholtz, W. G., Ewsuk, K. G., Ellerby, D. T. and Loehman, R. E., Near-net-shape processing of metal–ceramic composites by reactive metal penetration. *J. Am. Ceram. Soc.*, 1996, **79**, 2497–2499.
9. Fahrenholtz, W. G., Ewsuk, K. G., Loehman, R. E. and Tomsia, A. P., Formation of structural intermetallics by reactive metal penetration of Ti and Ni oxides and aluminates. *Metall. Mater. Trans. A*, 1996, **27**, 2100–2104.
10. Loehman, R. E., Ewsuk, K. and Tomsia, A. P., Synthesis of Al_2O_3–Al composites by reactive metal penetration. *J. Am. Ceram. Soc.*, 1996, **79**, 27–32.
11. Fahrenholtz, W. G., Ewsuk, K. G., Loehman, R. E. and Lu, P., Kinetics of ceramic–metal composite formation by reactive metal penetration. *J. Am. Ceram. Soc.*, 1998, **81**, 2533–2541.
12. Lu, P., Du, T. B., Loehman, R. E., Ewsuk, K. G. and Fahrenholtz, W. G., Interfacial microstructure formed by reactive metal penetration of Al into mullite. *J. Mater. Res.*, 1999, **14**, 3530–3537.
13. Lu, P., Loehman, R. E., Ewsuk, K. G. and Fahrenholtz, W. G., Transmission electron microscopy study of interfacial microstructure formed by reacting Al–Mg alloy with mullite at high temperature. *Acta Mater.*, 1999, **47**, 3099–3104.
14. Fahrenholz, W. G., Ellerby, D. T., Ewsuk, K. G. and Loehman, R. E., Forming Al_2O_3–Al composites with controlled compositions by reactive metal penetration of dense aluminosilicate preforms. *J. Am. Ceram. Soc.*, 2000, **83**, 1293–1295.
15. Saiz, E., Tomsia, A. P., Loehman, R. E. and Ewsuk, K. G., Effects of composition and atmosphere on reactive metal penetration of aluminium in mullite. *J. Eur. Ceram. Soc.*, 1996, **16**, 275–280.
16. Saiz, E. and Tomsia, A. P., Kinetics of metal–ceramic composite formation by reactive penetration of silicates with molten aluminium. *J. Am. Ceram. Soc.*, 1998, **81**, 2381–2393.
17. Saiz, E., Foppiano, S., MoberlyChan, W. and Tomsia, A. P., Synthesis and processing of ceramic–metal composites by reactive metal penetration. *Compos. Part A*, 1999, **30**, 399–403.

18. Liu, W. and Köster, U., Criteria for formation of interpenetrating oxide/metal composites by immersing sacrificial oxide preforms in molten metals. *Scripta Mater.*, 1996, **35**, 35–40.
19. Liu, W. and Köster, U., Fabrication of ceramic/metal composites by reduction of glass SiO_2 preforms in molten metals and alloys. *J. Mater. Sci. Lett.*, 1996, **15**, 2188–2191.
20. Liu, W. and Köster, U., Microstructures and properties of interpenetrating alumina/aluminium composites made by reaction of SiO_2 glass preforms with molten aluminium. *Mater. Sci. Eng. A*, 1996, **210**, 1–7.
21. Ceschini, L., Daehn, G. S., Garagnani, G. L. and Martini, C., Friction and wear behaviour of C^4 Al_2O_3/Al composites under dry sliding conditions. *Wear*, 1998, **216**, 229–238.
22. Imbeni, V., Hutchings, I. M. and Breslin, M. C., Abrasive wear behaviour of an Al_2O_3–Al co-continuous composite. *Wear*, 1999, 233–235, 462–467.
23. Badini, C., Puppo, D. and Pavese, M., Processing of co-continuous ceramic composites by reactive penetration method: influence of composition of ceramic preforms and infiltrating alloys. *Int. J. Mater. Product Tech.*, 2002, **17**, 182–204.
24. Badini, C., Breslin, M., Ceschini, L. and Landi, E., Analisi termiche differenziali e dilatometriche su materiali compositi co-continui (differential thermal and dilatometric analyses on co-continuous composite materials). *La Metallurgia Italiana*, 2000, **5**, 49–55.
25. La Vecchia, G. M., Badini, C., Puppo, D. and D'Errico, F., Co-continuous Al/Al_2O_3 composite produced by liquid displacement reaction: relationship between microstructure and mechanical behaviour. *J. Mater. Sci.*, 2003, **38**, 3567–3577.
26. Li, J. Q. and Xiao, P., Joining alumina using an alumina/metal composite. *J. Eur. Ceram. Soc.*, 2002, **22**, 1225–1233.
27. Yoshikawa, N., Watanabe, Y., Matamoros Veloza, Z., Taniguchi, S. and Kikuchi, A., Mechanical properties of Al/Al_2O_3composites fabricated by reaction between SiO_2 and molten Al, Al–Cu. *J. Mater. Sci. Lett.*, 1997, **16**, 1547–1550.
28. Yoshikawa, N., Kikuchi, A. and Taniguchi, S., Anomalous temperature dependence of the growth rate of the reaction layer between silica and molten aluminium. *J. Am. Ceram. Soc.*, 2002, **85**, 1827–1834.
29. Yoshikawa, N., Hattori, A. and Taniguchi, S., Growth rates and microstructures of reacted layers between molten Al–Fe alloy and SiO_2. *Mater. Sci. Eng. A*, 2003, **342**, 51–57.
30. Ha, C.-G., Jung, Y.-G. and Paik, U., Effect of microstructure on fracture behaviour of Al_2O_3/Al composite by reactive metal penetration. *J. Alloys Compd.*, 2000, **306**, 292–299.
31. Yun, Y. H., Hong, S. W. and Choi, C., Metal penetration processing and mechanical properties of Al/Al_2O_3 composite system. *J. Mater. Sci. Lett.*, 2002, **21**, 1297–1299.
32. Banerjee, S. and Roy, S. K., Net-shape forming of bi-continuous Al_2O_3/Al composite by displacement reaction. *Mater. Chem. Phys.*, 2001, **67**, 243–248.
33. Pavese, M., Fino, P., Valle, M. and Badini, C., Preparation of C4 ceramic/metal composites by reactive metal penetration of commercial ceramics. *Compd. Sci. Tech.*, 2006, **66**, 350–356.
34. Pavese, M., Puppo, D. and Badini, C., Compositi metallo-ceramici co-continui ottenuti per infiltrazione reattiva di preforme ceramiche (co-continuous metal–ceramic composites obtained by reactive infiltration of ceramic preforms). In *In Atti del 6 Congresso AIMAT*, 2002.
35. Pavese, M., Composites based on inorganic materials: co-continuous composites and multilayered ceramics. PhD thesis, Politecnico di Torino, Torino, Italy, 2003.
36. Standard UNI 9724:1990, Determinazione della massa volumica apparente e del coefficiente di imbibizione (Part 2). Determinazione della massa volumica reale e della porosità totale e accessibile (Part 7).
37. Gupta, S. V., *Practical density measurement and hydrometry*. IOP, London, 2002.
38. Boccaccini, A. R., Ondracek, G., Mazilu, P. and Windelberg, D., On the effective Young's modulus of elasticity for porous materials: microstructure modelling and comparison between calculated and experimental values. *J. Mech. Behav. Mater.*, 1993, **4**, 119–128.
39. Raj, R. and Thompson, L. R., Design of the microstructural scale for optimum toughening in metallic composites. *Acta Metall. Mater.*, 1994, **42**, 4135–4142.